

A boosted muon collider

Daniele Barducci, Alessandro Strumia

Dipartimento di Fisica, Università di Pisa, Italia

Abstract

A muon collider could produce the heavier Standard Model particles with a boost, for example in resonant processes such as $\mu^- \mu^+ \rightarrow h$ or $\mu^- \mu^+ \rightarrow Z$. We propose machine configurations that produce the boost (asymmetric beam energies, tilted beams) and estimate how much the luminosity is reduced or perhaps enhanced. The feasibility of the proposed configurations, as well as an estimation of the beam-induced backgrounds and beam energy spread, needs to be evaluated in order to derive more solid conclusions on the physics potential of such boosted collider configurations. If achievable, the boost can provide new interesting observational opportunities. For example it can significantly enhance the sensitivity to long-lived new particles decaying in a far-away detector, such as dark higgses or sterile neutrinos produced in h or Z decays.

Contents

1	Introduction	2
2	Boosting collisions at a muon collider	3
3	Resonant $\mu^- \mu^+ \rightarrow h$ production	6
4	Resonant $\mu^- \mu^+ \rightarrow Z$ production	9
5	Non resonant production of long-lived particles	11
6	Conclusions	11

1 Introduction

The luminosity of e^-e^+ circular colliders, even with 100 km length, strongly decreases with their energy above 100 GeV [1, 2]. So e^-e^+ colliders maximise the collision energy by performing symmetric head-on collisions with $\sqrt{s} \simeq 2E_{\text{beam}}$. On the other hand, the luminosity of $\mu^-\mu^+$ circular colliders grows roughly quadratically with their energy [3–5] and would allow to produce the heavier SM particles Z, h , etc using a smaller radius $R = E_{\text{beam}}/eB \approx 33 \text{ m} (E_{\text{beam}}/100 \text{ GeV})(10 \text{ T}/B)$, where B is the collider magnetic field.

Overall, at $\sqrt{s} = M_Z$ an e^-e^+ collider is expected to achieve a larger luminosity than a $\mu^-\mu^+$ collider. A $\mu^-\mu^+$ collider is nevertheless considered interesting at $\sqrt{s} = M_h$ (because the muon Higgs Yukawa coupling allows for $\mu^-\mu^+ \rightarrow h$ resonant Higgs production [6]) and at $\sqrt{s} = 2M_t$ (because low luminosity is enough for a precise measurement of the top quark mass [7]). However $\mu^-\mu^+$ colliders with energy below the TeV are challenging both from the point of view of the machine and detector design and the high level of background. Moreover, producing an on-shell resonant Higgs requires a beam energy spread comparable to its width over mass ratio, around 10^{-5} . While engineering such tiny energy spread might perhaps be possible, it poses a challenge for the accelerator design that needs to be addressed [6, 4].

We here explore the possibility that variations from the optimal symmetric head-on collision geometry could be interesting at a muon collider.

One technique, used in the PEP-II and KEK B e^-e^+ colliders at GeV-scale energy, employs head-on collisions of two beams with asymmetric energies E_+ and E_- , such that $s \simeq 4E_+E_-$. This generically allows to produce boosted particles, and was used to resonantly produce $e^-e^+ \rightarrow \Upsilon$. A muon collider could resonantly produce one heavy SM particle with given boost, such as $\mu^-\mu^+ \rightarrow Z$ or $\mu^-\mu^+ \rightarrow h$. In section 2 we explore how different $\mu^-\mu^+$ collision geometries can affect the luminosity. Asymmetric head-on collisions give a mild luminosity loss, while tilted collisions (discussed in [8] for a e^-e^+ collider) could allow to produce boosted heavy SM particles with enhanced luminosity, if a dedicated non-standard beam optics can be invented. We do not investigate the technical feasibility of these machines configurations and the related interaction regions, which need to be evaluated by accelerator and experimental experts, concentrating our study on identifying interesting physics cases that can take advantage of these non-standard collider options.

In particular, we show how the production of boosted heavy SM particles offers a significantly enhanced sensitivity to searches for long-lived weakly interacting new particles, as the boosted kinematics allows to concentrate them towards a far-away detector, that can only cover a small solid angle. Section 3 studies the case of resonant $\mu^-\mu^+ \rightarrow h$ Higgs production, section 4 studies $\mu^-\mu^+ \rightarrow Z$, section 5 considers generic non-resonant processes.

Various experimental effects must be thoroughly studied in order to assess the robustness of our results. Beam-induced background effects, that might have a significant impact in the forward-direction even if the detector is positioned far-away from the interaction point, must be investigated, together with beam-energy spread effects that might deplete the resonant cross-section for h, Z production.

Conclusions are given in section 6.

2 Boosting collisions at a muon collider

We here discuss the luminosity of two beams of particles with energies E_+ and E_- , masses m_+ and m_- that collide with relative angle θ between their spatial momenta \vec{p}_+ and \vec{p}_- , such that the collision energy is

$$s \equiv (p_+^\mu + p_-^\mu)^2 = 2 \left(E_+ E_- - |\vec{p}_+| |\vec{p}_-| \cos \theta + \frac{m_+^2 + m_-^2}{2} \right) \quad (1)$$

where $p_\pm^\mu = (E_\pm, \vec{p}_\pm)$ are the quadri-momenta.

2.1 Head-on collisions with asymmetric beam energies

The collision energy s is maximal in the usual case of head-on collisions, corresponding to $\theta = \pi$. We consider two μ^\pm beams with energies $E_\pm = \gamma_\pm m_\mu$ circulating in rings with radii R_\pm , and thereby with magnetic fields $B_\pm = E_\pm / R_\pm e$, containing $N_{b\pm}$ bunches of N_\pm muons μ^\pm each. In order to collide, the bunches must be equi-spaced, $R_+ / N_{b+} = R_- / N_{b-}$. We denote as f the repetition rate of acceleration cycles. The instantaneous luminosity can be straightforwardly computed by adapting the standard computation of, e.g., [9] to the general case. By considering the fact that the beams have an asymmetric configuration one obtains

$$\mathcal{L} = \frac{f N_+ N_-}{2\pi(\sigma_{T+}^2 + \sigma_{T-}^2)} \sum_{j=0}^{\infty} \exp\left(-\frac{2\pi R_+}{\gamma_+ \tau_\mu N_{b+}} j\right) \exp\left(-\frac{2\pi R_-}{\gamma_- \tau_\mu N_{b-}} j\right). \quad (2)$$

By summing the geometric series and expanding the exponential one thus arrives at

$$\mathcal{L} = \frac{\tau_\mu}{R_+ / \gamma_+ N_{b+} + R_- / \gamma_- N_{b-}} \frac{f N_+ N_-}{(2\pi)^2 (\sigma_{T+}^2 + \sigma_{T-}^2)}, \quad (3)$$

where τ_μ is the μ lifetime and $\sigma_{T\pm}$ are the bunches transverse sizes. This expression reduces to the usual luminosity for beams of unstable particles in the symmetric case [9]. Head-on symmetric collisions with $E_+ \neq E_-$ have suppressed instantaneous luminosity compared to the symmetric case $E_+ = E_-$ with the same s , because of two factors:

1. the first term of eq. (3) implies that the muons with lower energy (say E_-) decay faster than those with higher energy, not allowing to use the more boosted life-time to gain luminosity;
2. the transverse bunch sizes $\sigma_{T\pm}$ in the second term of eq. (3) are given by

$$\frac{1}{\sigma_{T\pm}^2} = \frac{E_\pm^2 f_{\text{hg}} \sigma_{\delta\pm}}{m_\mu \epsilon_{L\pm} \epsilon_{T\pm}}, \quad (4)$$

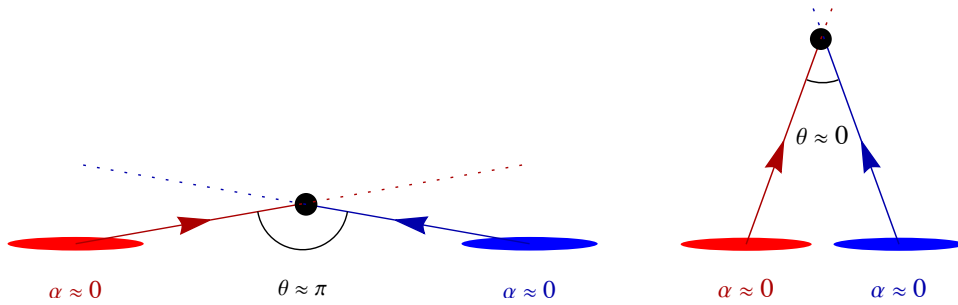


Figure 1: **Left:** the usual nearly-head-on collision geometry, where the luminosity is increased by tilting the bunches by a small angle. **Right:** the collision geometry that could enhance the luminosity of processes such as $\mu^+\mu^- \rightarrow h$ with $E \gg M_h$.

where $\sigma_{\delta_{\pm}}$ is the fractional beam energy spread, $f_{\text{hg}} \approx 0.76$ is the hourglass factor [10, 9] that limits the maximal focusing achievable, and $\epsilon_{L,T}$ are the longitudinal and transverse emittances of the bunches, roughly conserved during the acceleration process. This means that a higher-energy beam can be better focused, but this gain is lost when colliding it with a thicker lower energy beam (say $\sigma_{T-} \gg \sigma_{T+}$).

As a result, by using eq. 3, the luminosity at fixed s gets reduced as

$$\frac{\mathcal{L}(E_+ \neq E_-)}{\mathcal{L}(E_+ = E_-)} = \frac{2E_+E_-}{E_+^2 + E_-^2} = \frac{1}{2\gamma^2 - 1} \quad (5)$$

in the limit of equal quality beams, $\epsilon_{L+} = \epsilon_{L-}$, $\epsilon_{T+} = \epsilon_{T-}$, $\sigma_{\delta+} = \sigma_{\delta-}$. The luminosity loss can be mitigated if, e.g., the lower energy beam has larger energy spread (say $\sigma_{\delta-} > \sigma_{\delta+}$). The latter term in eq. (5) shows the result as function of the boost factor $\gamma \geq 1$ of a resonantly produced particle $\mu^-\mu^+ \rightarrow X$. As discussed in the next sections, the boost γ enhances the sensitivity of specific searches, partially compensating for this luminosity loss.

2.2 Rear-end collisions with asymmetric beam energy

Rear-end collisions among beams circulating in the same direction (corresponding to $\theta = 0$) allow to reduce \sqrt{s} while keeping comparable beam energies. This collision geometry has two problems. First, $s \simeq m_{\mu}^2[2 + (E_+^2 + E_-^2)/E_+E_-]$ is too low if one wants to produce the heavier SM particles rather than GeV-scale particles. Second, the collision region is too long, $\sigma_L/\delta v$, where $\sigma_L \sim \text{mm}$ is a realistic beam length [4] and $\delta v \simeq (1/\gamma_-^2 - 1/\gamma_+^2)/2$ for $\gamma_{\pm} \gg 1$ is the small relative velocity.

2.3 Oblique collisions with equal beam energy

In order to reduce the collision energy of eq. (1) by the desired amount compared to the beam energies we consider oblique collisions with generic angle θ . For $E_{\pm} \gg \sqrt{s}$ one needs $\theta \ll 1$, and eq. (1) reduces to $s \simeq E_+ E_- \theta^2$, where θ is expressed in radians. Collisions are then dominantly due to the transverse relative velocity between beams. We here compute the luminosity for generic θ . Assuming Gaussian bunches with equal longitudinal bunch sizes σ_L and equal transverse beam sizes σ_T implies that the tilt angle affects the luminosity as [11]

$$\frac{\mathcal{L}(\theta)}{\mathcal{L}(\pi)} = \left[1 + \frac{\sigma_L^2}{\sigma_T^2} \cot^2 \frac{\theta}{2} \right]^{-1/2} \quad (6)$$

where $\mathcal{L}(\pi)$ corresponds to maximal s . Bunches are usually focused such that $\sigma_T \ll \sigma_L$ at the collision point (planned values are $\sigma_T \sim \mu\text{m}$ and $\sigma_L \sim \text{mm}$ [4]), so even a small deviation from head-on $|\theta - \pi| \gtrsim \sigma_T/\sigma_L$ causes a significant drop in luminosity. This can be avoided by colliding in a crab-like configuration [12,13] by tilting the bunches in order to recover the missing geometric overlap. We define the crabbing angle α as the angle between the longitudinal size of the bunches σ_L and the direction identified by the difference of the bunches spacial momenta. The zero-tilting case of eq. (6) (with σ_L along the beam axis) corresponds to $\alpha = (\pi - \theta)/2$. The optimal collision geometry, with bunches rotated in the way illustrated in both panels of fig. 1, is obtained for $\alpha = 0$:

$$\frac{\mathcal{L}(\theta, \alpha)}{\mathcal{L}(\pi, 0)} = \sqrt{\frac{1 - \cos \theta}{1 + \frac{\sigma_L^2}{\sigma_T^2} - \left(1 - \frac{\sigma_L^2}{\sigma_T^2}\right) \cos \alpha}} = \sin \frac{\theta}{2} \quad \text{for } \alpha = 0 \quad (7)$$

A muon collider collision with reduced s (for example $\sqrt{s} = M_h$ when considering $\mu^- \mu^+ \rightarrow h$) can be obtained from beams with equal energy $E_{\pm} = E \gg m_{\mu} = m_{\pm}$ choosing the collision angle θ as

$$\theta = \arccos \left(1 - \frac{s}{2E^2} \right), \quad (8)$$

so that $\sqrt{s} \ll E$ is obtained from a small $\theta \simeq \sqrt{s}/E$, corresponding to quasi-parallel beams. In this limit eq. (6) reduces to $\mathcal{L}(\theta)/\mathcal{L}(\pi) \simeq (\theta/2)(\sigma_T/\sigma_L)$: the double suppression by $\theta \ll 1$ and by $\sigma_T/\sigma_L \ll 1$ implies a big luminosity loss with the usual geometry of beams. The latter suppression is avoided colliding tilted bunches with the optimal angle $\alpha = 0$, such that eq. (7) reduces to

$$\frac{\mathcal{L}(\theta, \alpha)}{\mathcal{L}(\pi, 0)} \simeq \frac{\theta}{2} \simeq \frac{1}{\gamma}. \quad (9)$$

This suppression in the luminosity is milder than the enhancement $\mathcal{L}(\pi, 0) \propto E^2$ of the luminosity of a $\mu^- \mu^+$ circular collider as its beam energy E is increased. So a $\mu^- \mu^+$ circular collider with nearly-parallel beams of energy E could potentially produce heavier SM particles of mass $\sqrt{s} = M$ with luminosity enhanced by $\gamma = 2E/M$ compared to usual head-on collisions with

$E = M/2$.¹ However this would need a dedicated machine optics with the beam geometry illustrated in the right panel of fig. 1 to achieve $\alpha \approx 0$. It could be interesting to explore if this can be realistically realized. A pre-collision region with a time-dependent magnetic field in a size $2R'$ could rotate conventional head-on beams by nearly $\pm 90^\circ$ without rotating the bunches, providing collisions with $\sqrt{s} = eBR'$ (e.g. $\sqrt{s} = M_h$ $R' = M_h/eB = 42$ m for $B = 10$ T), but the real difficulty is achieving focus at the collision point. With this geometry the beam energy spread σ_δ negligibly contributes to the spread in \sqrt{s} , that is produced in the rotation process. We do not explore if/how these wild speculations could be realistically implemented.

Even if this luminosity gain cannot be practically achieved, the boosted produced particles lead to the extra gain in the sensitivity of some specific searches discussed in the next sections. So even the simpler option of limiting the luminosity loss as in section 2.1 could be interesting. We thus explore in the following sections the physics potential of such collider configurations with beam energies ranging from $E_\pm = E_{h,Z}/2$ up to $E_\pm = 5$ TeV.

3 Resonant $\mu^- \mu^+ \rightarrow h$ production

We consider $\mu^- \mu^+ \rightarrow h$ resonant production of Higgs bosons with boost $\gamma_h = E_h/M_h$. As discussed in section 2, this could be done at a muon collider with luminosity possibly reduced by $\sim 1/\gamma_h^2$ or perhaps enhanced by γ_h . As mentioned in the Introduction, producing an on-shell resonant Higgs requires a small beam energy spread $\sim \Gamma_h/M_h \sim 10^{-5}$, which poses a challenge for the accelerator design [4] but that, if overcome, can lead to interesting physics possibilities [6]. Around the Higgs peak one expects

$$\sigma(\mu^- \mu^+ \rightarrow h \rightarrow X) = \frac{4\pi\Gamma_h^2 \text{BR}(h \rightarrow \mu^- \mu^+)}{(s - M_h^2)^2 + M_h^2\Gamma_h^2} \text{BR}(h \rightarrow X) . \quad (10)$$

Here $\Gamma_h/M_h \approx 3 \times 10^{-5}$ is the narrow Higgs width, and $\text{BR}(h \rightarrow \mu^- \mu^+) \approx 0.22 \times 10^{-3}$ in the SM. Then the peak cross section would be $\sigma(\mu^- \mu^+ \rightarrow h) = 4\pi \text{BR}(h \rightarrow \mu\mu)/M_h^2 \approx 71$ pb. Initial state radiation reduces it down to $\sigma \approx 37$ pb, and the unknown energy beam spread could further reduce it down to $\sigma \approx 22$ pb [14]. We here assume this latter value. This is comparable to the Higgs production cross section at a pp collider, $\sigma(pp \rightarrow h) \sim 50$ pb at $\sqrt{s} = 13$ TeV, dominated by $gg \rightarrow h$.

We here discuss what can be gained by having boosted Higgses, produced in the configuration of the right panel of fig. 1. The main new qualitative feature is that most final states from Higgs decay are in a small forward cone — a region near to the beam pipe that is particularly problematic at a muon collider. This would affect generic measurements allowing, for example, to independently measure the Higgs mass from the angular distribution of its decay products.

The focusing feature become advantageous when performing specific searches for particles ϕ (for example hypothetical scalars ϕ produced in $h \rightarrow \phi\bar{\phi}$ decays and dubbed ‘dark Higgs

¹Since a muon collider matches the scaling $\sigma \propto 1/E$ of bunch size with particle wave-length, the scaling factor γ can be also obtained from the simpler problem of colliding two particles: γ arises as the factor $t_{\text{cm}} = \gamma t_{\text{lab}}$ that relates the collision time in the laboratory and center-of-mass frames.

bosons') that are long-lived and interact weakly with SM particles in the crossed surrounding material, producing a visible final state away from the collision point when they decay or scatter with the material. The advantage arises because a detector away from the collision point can only cover a small angular size Ω around the collision. It is thereby convenient that the Higgs boost concentrates all ϕ arising from its decay in a small cone with $\Omega \simeq \pi\theta_\phi^2$, where θ_ϕ is the ϕ polar angle with respect to the Higgs direction in the laboratory frame. Placing the detector in the decay cone allows to gain sensitivity. The gain factor is limited when considering a detector sensitive to ϕ particles that decay or scatter only within its volume, as its sensitivity is maximal when placed at a distance from the collision point comparable to the size of the detector itself, even if the boosted ϕ life-time is much longer. We will consider a cylindrical detector placed at 70 m distance, with 50 m length and with 3 m radius.

We now compute the sensitivity on long-lived particles from Higgs decay showing that it can be a few orders of magnitude better than the sensitivity of a similar detector with a similar luminosity at the LHC pp collider, as well as than at a symmetric muon collider. We consider the specific example of a $h \rightarrow \phi\bar{\phi}$ decay, where ϕ can be a SM particle or an hypothetical new particle with mass $M_\phi < M_h/2$. The ϕ particles tend to be concentrated along the Higgs direction. The Higgs has spin 0, so $h \rightarrow \phi\bar{\phi}$ is isotropic in the Higgs rest frame. The angular distribution in the laboratory frame in terms of $\epsilon = 2M_\phi/M_h$ and $X = \cos^2\theta_\phi(\gamma_h^2 - 1) - \gamma_h^2$ is

$$\frac{dN_\phi}{d\cos\theta_\phi} = \frac{X(1 + \epsilon^2\gamma_h^2) + 2\gamma_h \left[\gamma_h + \cos\theta_\phi \sqrt{(\gamma_h^2 - 1)(1 + X\epsilon^2)} \right]}{2X^2 \sqrt{(1 - \epsilon^2)(1 + X\epsilon^2)}} \simeq \frac{2\gamma_h^2}{(1 + \gamma_h^2\theta_\phi^2)^2} \quad (11)$$

normalized such that $dN_\phi/d\cos\theta_\phi = 1/2$ for $\gamma_h = 1$. The latter expression in eq. (11) holds in the forward limit $\theta_\phi \ll 1/\gamma_h$ for large $\gamma_h \gg 1$ and, for simplicity, light ϕ particles $\epsilon \ll 1$. It shows that the angular distribution is concentrated in the forward direction $\theta_\phi = 0$ within an angle $\theta_\phi \sim 1/\gamma_h$. Furthermore, if $\epsilon\gamma_h > 1$ (namely if $E_h > M_h^2/2M_s$) all ϕ particles are within the cone $\theta_\phi < \theta_{\max}$, found by imposing $1 + X\epsilon^2 = 0$:

$$\tan^2\theta_{\max} = \frac{M_h^2 - 4M_s^2}{4\gamma_h^2 M_\phi^2 - M_h^2}. \quad (12)$$

The angular distribution, shown in the left panel of fig. 2, peaks at $\theta_\phi = 0$, and also features a narrow Jacobian peak at the maximal value $\theta_\phi = \theta_{\max}$ for $\sqrt{s} = 10$ TeV (black curve). For comparison, the left panel of fig. 2 also shows the flatter analogous distribution that arises from $\mu^- \mu^+ \rightarrow VV \rightarrow h$ vector-boson-fusion production at a symmetric muon collider with $s \gg M_h^2$ (dot-dashed red), and from $pp \rightarrow h$ production at the LHC collider, considering the $gg \rightarrow h$ dominant production mode (dashed red).

The resulting sensitivity is shown in the right panel of fig. 2, as limits on the Higgs exotic branching ratio (BR) versus the proper ϕ decay length $c\tau$. We assume the reconstruction efficiency of the ϕ decay products to be 100% and we work in the zero background hypothesis, as usually done for these types of studies. We consider a far-away detector with $\approx 2000 \text{ m}^3$

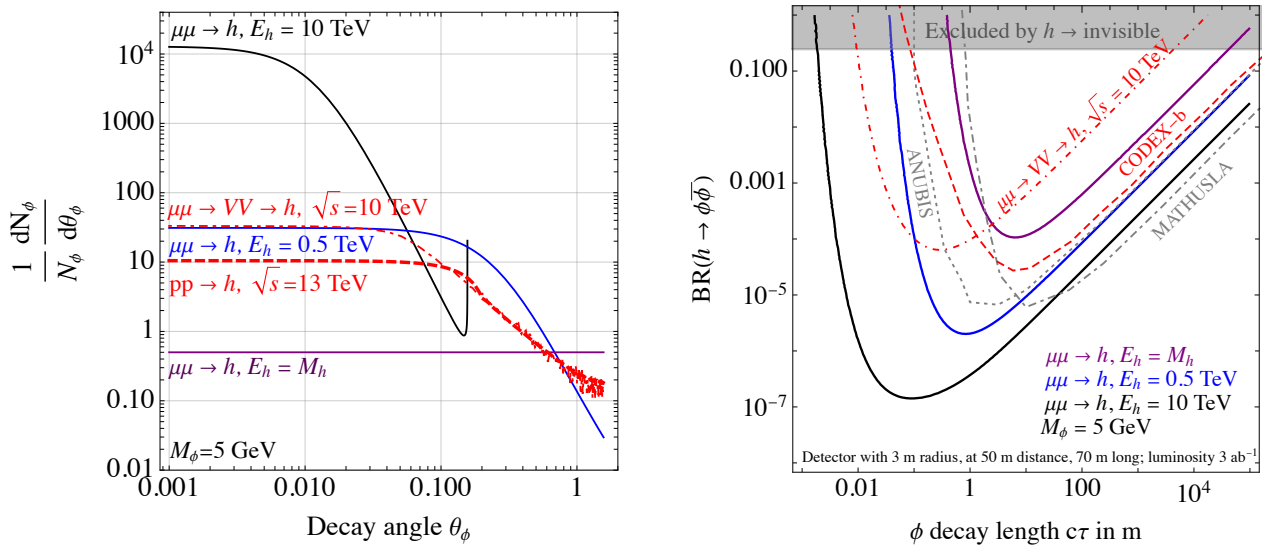


Figure 2: **Left:** Angular distribution of ϕ particles per one $h \rightarrow \phi\bar{\phi}$ decay. We consider the Higgs h produced as $\mu^- \mu^+ \rightarrow h$ at a boosted muon collider, as $\mu^- \mu^+ \rightarrow VV \rightarrow h$ at a symmetric muon collider, as $pp \rightarrow h$ at the LHC collider with $\sqrt{s} = 13 \text{ TeV}$. So a boosted muon collider can produce much higher fluxes in the forward direction $\theta_\phi \ll 1$. **Right:** the resulting sensitivities, taking into account the cross sections $\sigma(\mu^- \mu^+ \rightarrow h) \approx 22 \text{ pb}$, $\sigma(\mu^- \mu^+ \rightarrow VV \rightarrow h) \approx 0.85 \text{ pb}$, $\sigma(pp \rightarrow h) \approx 50 \text{ pb}$, and considering a far-away detector with $\sim 2000 \text{ m}^3$ volume, such as CODEX-B [15]. At given luminosity, a boosted $\mu^- \mu^+ \rightarrow h$ collider offers a much higher sensitivity than a symmetric muon collider and than LHC. For comparison we also show the sensitivity of larger far-away detectors ANUBIS (about 6 times larger volume [16], see also [17] for a recent design proposal) and MATHUSLA (about 130 times larger [18]).

volume, comparable to the CODEX-B detector being discussed for the LHC [15]. Our results are illustrated in black, blue and purple for $E_h = 10 \text{ TeV}$, 500 GeV and M_h respectively. LHC and a symmetric muon collider (dot-dashed red) offer similar sensitivity at similar luminosity, given that the cross sections are similar. On the other hand, boosted Higgs production at a muon collider allows to improve the sensitivity by a few orders of magnitude, outperforming even larger detectors such as ANUBIS [16] and MATHUSLA [18] being discussed for the LHC. Furthermore, the boost would allow to observe events with both particles ϕ within the forward detector, providing additional information, such as the differential time-of-flight.

Fig. 2 right assumes $M_\phi = 5 \text{ GeV} \ll M_h$. An even larger sensitivity enhancement arises if instead M_ϕ is just a little below $M_h/2$. In such a case θ_{max} in eq. (12) gets smaller, meaning that all particles ϕ get concentrated in a smaller cone at a boosted μ collider. A longer thinner detector with the same volume would allow to exploit this feature, offering further enhanced sensitivity.

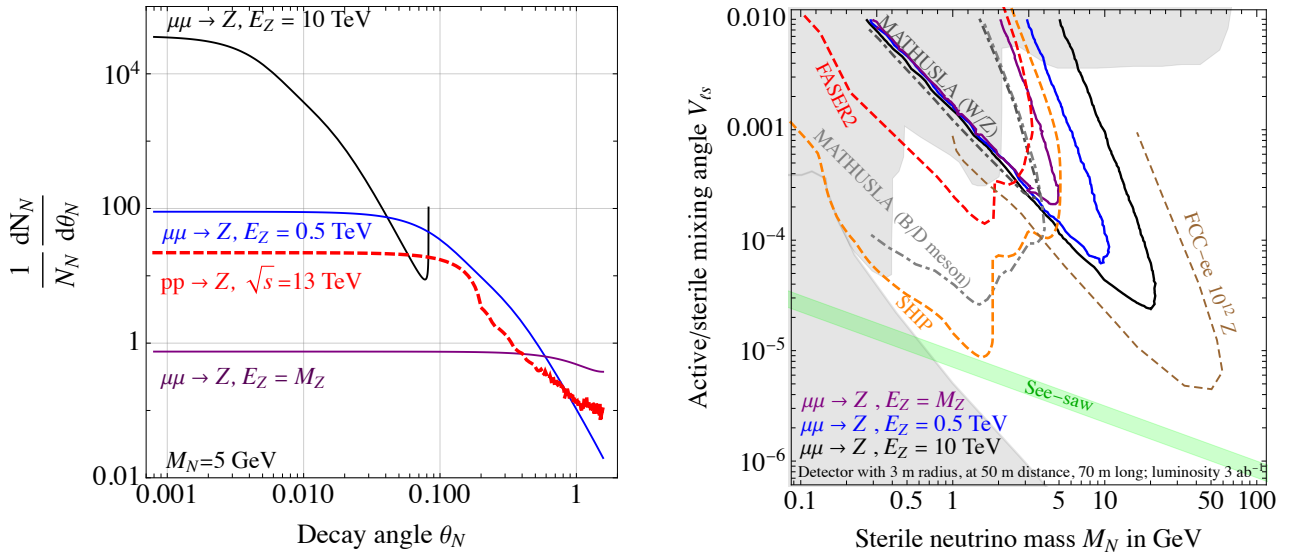


Figure 3: **Left:** Angular distribution of N particles per one $Z \rightarrow N\nu$ decay. We consider the Z produced as $\mu^- \mu^+ \rightarrow Z$ at a boosted muon collider, as $pp \rightarrow Z$ at the LHC collider with $\sqrt{s} = 13 \text{ TeV}$. **Right:** the resulting sensitivities, taking into account the cross sections $\sigma(\mu^- \mu^+ \rightarrow Z) \approx 6 \times 10^4 \text{ pb}$ and considering the same experimental setup of fig. 2. For comparison we also show the sensitivity of other proposed experiments as well as the existing bounds from terrestrial analyses and astrophysics (in gray), all taken from [19].

4 Resonant $\mu^- \mu^+ \rightarrow Z$ production

Similar signals to those discussed in section 3 arise substituting the Higgs h with the Z boson as the resonantly produced particle that decays into new long-lived states. We focus on the differences. The peak cross section is higher,

$$\sigma(\mu^- \mu^+ \rightarrow Z) = 3 \, 4\pi \text{BR}(Z \rightarrow \mu^- \mu^+) / M_Z^2 \approx 60 \times 10^3 \text{ pb}, \quad (13)$$

in view of $\text{BR}(Z \rightarrow \mu^- \mu^+) \approx 0.0337$. Furthermore, as the Z has a larger width $\Gamma_Z \approx 2.49 \text{ GeV} \gg \Gamma_h$, on-shell Z production is easily achieved, and losses due to initial state radiation can be neglected. The factor 3 in eq. (13) arises because the Z boson has spin 1. For the same reason, Z decays need not being isotropic in the Z rest frame. We thereby consider specific new-physics models, where the three key phenomenological parameters (mass and decay length of the new long-lived particle, and Z -boson branching ratio into the new particle) are computed in terms of model parameters.

A plausible theory where the Z boson decays into a long-lived particle is the SM extended with a fermion singlet N with mass M_N , dubbed ‘right-handed’ or ‘sterile neutrino’ because it can have the Yukawa couplings $y_\ell L_\ell N H$ to left-handed leptons L_ℓ and to the Higgs doublet H . Once H acquires its vacuum expectation value v , this coupling produces a mass mixing

$V_{\ell s} \simeq y_\ell v/M_N \ll 1$ with SM neutrinos, and a contribution $(m_\nu)_{\ell\ell'} = V_{\ell s} V_{\ell' s} M_N$ to their mass matrix, motivating small values of $V_{\ell s}$ that result in a long-lived N . The main N decay rates are [20, 21]

$$\Gamma(N \rightarrow \ell\bar{\ell}'\nu_{\ell'}, \ell q\bar{q}) \sim \frac{G_F^2 M_N^5}{96\pi^3} |V_{\ell s}|^2, \quad \Gamma(N \rightarrow \pi^0 \nu_\ell) \sim \frac{G_F^2 M_N^3 f_\pi^2}{32\pi} |V_{\ell s}|^2. \quad (14)$$

Therefore the life-time $\tau_N = 1/\Gamma_N$ steeply scales with M_N . On the other hand, the Z -boson decay rate dominantly depends on the mixing [22]

$$\text{BR}(Z \rightarrow \nu N) \simeq \text{BR}(Z \rightarrow \nu\nu) \frac{2}{3} \sum_\ell |V_{\ell s}|^2 \left(1 - \frac{M_N^2}{M_Z^2}\right)^2 \left(1 + \frac{M_N^2}{2M_Z^2}\right) \quad (15)$$

where $\text{BR}(Z \rightarrow \nu\bar{\nu}) \approx 20.0\%$. The angular distribution of the sterile neutrino N produced in Z decays is shown in the left panel of fig. 3. This plot is similar to fig. 2, left panel, for Higgs decays, except that we have here omitted vector-boson-fusion $\mu^- \mu^+ \rightarrow Z$ production at a symmetric muon collider, in view of its small cross section, about 4 pb at $\sqrt{s} = 10$ TeV.

Constraints and sensitivities are presented in the right panel of fig. 3. We consider a far away detector with the same geometry (volume and distance) as in fig. 2, right panel, and we adopt the same assumptions on reconstruction efficiency and background. While fig. 2 was made in the phenomenological plane $(c\tau, \text{BR})$, fig. 3 uses the model parameters $(M_N, |V_{\ell s}|^2)$, possibly restricted along or below the green band where m_ν acquires the observed values (assuming either normal or inverted neutrino mass hierarchy). Using model parameters allows to consider a variety of different experiments: colliders, fixed target, meson decays. The various existing bounds are plotted as dark shadows, from [19]. The sensitivities of possible experiments are plotted as dashed curves: FASER2 [23] and the larger proposed detector MATHUSLA mostly look at decays of mesons produced at the LHC, while the proposed SHIP experiment would look at mesons produced by fixed-target collisions [19, 24]. We also show the reach of MATHUSLA [25] when looking at Z, W decays. A boosted muon collider offers a comparable reach on the mixing angle, but in a different region with larger mass M_N , since sterile neutrinos arise from boosted Z decays. Other proposed detectors such as ANUBIS and CODEX-B offer a comparable or weaker reach [26, 27], and we do not show them for clarity. The same consideration applies for similar far-detector at the proposed FCC-hh experiment, see *e.g.* [28].

Furthermore, Z bosons can also be resonantly produced at an e^-e^+ collider: a future circular e^-e^+ collider with 100 km length could perhaps produce 10^{12} Z bosons, corresponding to a $\mathcal{L} \sim 20/\text{ab}$ integrated luminosity [1, 2], larger than what assumed for a muon collider. Such a 100 km e^-e^+ collider, with a full 4π detector that captures all $Z \rightarrow \nu N$ decays (in the mass range where τ_N is not too large), offers higher sensitivity than the assumed boosted muon collider, with small-angle detector and lower luminosity. None of these proposals reaches the band denoted as ‘see-saw’, where the neutrino masses mediated by the sterile neutrino match the measured neutrino masses.

If multiple quasi-degenerate sterile neutrinos exist, a boost could help studying their oscillations, similarly to what done with mesons at e^-e^+ asymmetric colliders.

Similar results hold for different models, such as a new vector V produced as $Z \rightarrow \gamma V$.

5 Non resonant production of long-lived particles

The previous sections assumed that the SM h, Z particles act as mediators between muons and new long-lived states. This made convenient having a collider running at the resonance $\sqrt{s} = M_{h,Z}$ for h, Z production, rather than at the maximal possible \sqrt{s} .

More in general, mediators could be new unknown particles exchanged in the s or t channel: in such a case running at reduced $\sqrt{s} < 2E_{\text{beam}}$ around the unknown mediator masses would similarly enhance the sensitivity to long-lived particles.

If mediators are heavier than the collider energy, physics gets approximated via effective operators. In this idealised limit the cross sections for producing new long-lived light particles can grow with the collision energy, reducing the advantage of running a collider at \sqrt{s} below the maximal $\sqrt{s} = 2E_{\text{beam}}$. Let us consider two examples.

- A dimension 5 effective operator, such as a sterile neutrino N coupled to photons via a magnetic dipole moment operator $F_{\mu\nu}(\bar{\nu}\gamma_{\mu\nu}N)/\Lambda$. The resulting cross section $\sigma(\mu^- \mu^+ \rightarrow \gamma^* \rightarrow \nu N) \sim e^2/\Lambda^2$ is energy-independent [29], so considerations similar to previous sections apply.
- A dimension 6 effective operator, such as a sterile neutrino N coupled to SM fermions via $(\bar{\mu}\gamma_{\alpha}\mu)(\bar{\nu}\gamma^{\alpha}N)/\Lambda^2$ operators. In such a case the $\gamma^2 = E_{\text{beam}}^2/s$ enhancement of the N flux in the boosted direction gets compensated by the energy dependence of the production cross section $\sigma(\mu^- \mu^+ \rightarrow \nu N) \sim s/\Lambda^4$ (and possibly by the boosted decay length, if it exceeds the detector size). As a result a boosted collider would be convenient only if it could deliver an enhanced luminosity compared to a symmetric collider [30].

Rather than studying in the detail all possibilities, we conclude with a panoramic summary of the main points.

6 Conclusions

We explored the possibility of running a collider in ‘boosted’ configuration, with beam energies higher than the collision energy \sqrt{s} , thereby producing particles boosted by a factor $\gamma \approx E_{\text{beam}}/\sqrt{s}$. We considered producing the heavier SM particles, such as the Higgs and the Z boson. Their boosted production is not done at e^-e^+ colliders because it implies a big luminosity loss at fixed consumed power. The situation is different at a $\mu^- \mu^+$ collider, where the luminosity of head-on symmetric collisions is expected to grow proportionally to s . In section 2 we estimated that achieving a boost γ affects the luminosity as

$$\frac{\mathcal{L}_{\text{boosted}}}{\mathcal{L}_{\text{symmetric}}} \sim \begin{cases} 1/\gamma^8 & e^-e^+ \text{ head-on collisions with asymmetric beam energies,} \\ 1/\gamma^2 & \mu^- \mu^+ \text{ head-on collisions with asymmetric beam energies,} \\ \gamma & \mu^- \mu^+ \text{ oblique collision with same beam energies.} \end{cases} \quad (16)$$

Therefore the simplest head-on geometry gives a mild luminosity loss at a $\mu^- \mu^+$ collider, while a luminosity enhancement could potentially arise performing oblique collisions, if focused bunches

can be tilted by an appropriate large angle. While small-angle tilting is considered possible [31], a large angle would need a dedicated beam optics: whether this is possible or not is a key aspect beyond the scope of this work, which we do not investigate further. We instead concentrated on identifying interesting physics cases that can take advantage of these non-standard collider options.

Next, we explored what can be achieved by having boosted particles. The boost significantly helps one search for specific new physics: long-lived new particles that can be best detected in a far-away detector. The reason is that the far-away detector can only cover a relatively small solid angle $\Omega \ll 4\pi$ around the interaction point, and thereby placing it along the boost direction enhances the signal rate by a factor γ^2 , possibly reduced down to a factor γ if the particles are so much long-lived that boosted decays happen beyond the detector. Thereby the number of detected events, that controls the sensitivity of the search, scales as

$$\frac{N_{\text{boosted}}}{N_{\text{symmetric}}} \sim \gamma^{1-2} \frac{\mathcal{L}_{\text{boosted}}}{\mathcal{L}_{\text{symmetric}}} \frac{\sigma(E^2)}{\sigma(s)}. \quad (17)$$

The production cross sections can scale in different ways with energy, depending on the model. The main possibilities are:

$$\frac{\sigma(E^2)}{\sigma(s)} \sim \begin{cases} \gamma^2 & \text{Decays of } Z, h \text{ mediators, produced resonantly at } s = M_{h,Z}^2 \\ 1 & \text{Dimension 5 effective operators.} \\ 1/\gamma^2 & \text{Dimension 6 effective operators.} \end{cases} \quad (18)$$

The most optimistic win-win-win situation would provide a gain $N_{\text{boosted}}/N_{\text{symmetric}} \sim \gamma^5$ in the case where resonantly produced boosted Higgs bosons decay into mildly long-lived new particles, assuming that oblique collisions can enhance the luminosity of a $\mu^- \mu^+$ collider as in eq. (16). The boost factor could be $\gamma \sim E/M_h \sim 10$ or more. Fig. 2 shows that boosting the Higgs can provide higher sensitivity than other proposals, having assumed the same luminosity and a relatively small far detector, such as CODEX-B.

Analogously, section 4 studies Z decays into long-lived new particles and fig. 3 shows that a boosted $\mu^- \mu^+ \rightarrow Z$ collider can compete with other proposals.

We conclude by stressing that, in order to assess the robustness of our results, various experimental effects must be investigated further. These includes beam-induced background effects, that might have a significant impact in the forward-direction even if the detector is positioned far-away from the interaction point, together with beam-energy spread effects that might deplete the resonant cross-section for h, Z production.

Acknowledgments

This work was supported by the MIUR grant PRIN 2017L5W2PT. We thank Rama Calaga, Stephane Fartoukh, Roberto Franceschini Filip Moortgat, Eugenio Paoloni, Arsenii Titov and Andrea Wulzer for useful discussions on collider aspects.

References

- [1] X.C. Lou for the CEPC Collaboration, ‘*Circular e^\pm Collider — Status and Progress*’, talk at HKUST-IAS, 17/1/2022. See also the [CEPC web site](#).
- [2] FCC Collaboration, ‘*FCC Physics Opportunities*’, Eur.Phys.J.C 79 (2019) 474.
- [3] H. Al Ali et al., ‘*The muon smasher guide*’, Rept.Prog.Phys. 85 (2022) 084201 [[arXiv:2103.14043](#)].
- [4] MUON COLLIDER Collaboration, ‘*The physics case of a 3TeV muon collider stage*’ [[arXiv:2203.07261](#)].
- [5] D. Schulte, “*Muon Collider Parameters at different Energies*”. D. Schulte, “*Muon Collider*”.
- [6] J. de Blas, J. Gu, Z. Liu, ‘*Higgs boson precision measurements at a 125 GeV muon collider*’, Phys.Rev.D 106 (2022) 7, 073007 [[arXiv:2203.04324](#)].
- [7] R. Franceschini, A. Strumia, A. Wulzer, ‘*The collider landscape: which collider for establishing the SM instability?*’, JHEP 08 (2022) 229 [[arXiv:2203.17197](#)].
- [8] D. Fu, A. Ruzi, M. Lu, Q. Li, ‘*New methods to achieve meson, muon and gamma light sources through asymmetric electron positron collisions*’, Int.J.Mod.Phys.A 38 (2023) 2350033 [[arXiv:2211.05240](#)].
- [9] C. Accettura et al., ‘*Towards a Muon Collider*’ [[arXiv:2303.08533](#)].
- [10] W. Herr, B. Muratori, ‘*Concept of luminosity*’, Intermediate accelerator physics. Proceedings, CERN Accelerator School 361 (2003) .
- [11] T. Suzuki, “*General Formulas of Luminosity for Various Types of Colliding Beam Machines*”, KEK-76-3.
- [12] K. Oide, K. Yokoya, ‘*The Crab Crossing Scheme for Storage Ring Colliders*’, Phys.Rev.A 40 (1989) 315.
- [13] Y.-P. Sun, R. Assmann, J. Barranco, R. Tomas, T. Weiler, F. Zimmermann, R. Calaga, A. Morita, ‘*Beam dynamics aspects of crab cavities in the CERN Large Hadron Collider*’, Phys.Rev.ST Accel.Beams 12 (2009) 101002.
- [14] M. Greco, T. Han, Z. Liu, ‘*ISR effects for resonant Higgs production at future lepton colliders*’ [[arXiv:1607.032107](#)].
- [15] CODEX-b Collaboration, ‘*The Road Ahead for CODEX-b*’ [[arXiv:2203.07316](#)].
- [16] M. Bauer, O. Grandt, L. Lee, C. Ohm, ‘*ANUBIS: Proposal to search for long-lived neutral particles in CERN service shafts*’ [[arXiv:1909.13022](#)].
- [17] “*Update on (pro)ANUBIS detector proposal*”.
- [18] MATHUSLA Collaboration, ‘*A Letter of Intent for MATHUSLA: A Dedicated Displaced Vertex Detector above ATLAS or CMS.*’ [[arXiv:1811.00927](#)].
- [19] SHiP Collaboration, ‘*A facility to Search for Hidden Particles at the CERN SPS: the SHiP physics case*’, Rept.Prog.Phys. 79 (2016) 12, 124201 [[arXiv:1504.04855](#)].
- [20] D. Gorbunov, M. Shaposhnikov, ‘*How to find neutral leptons of the ν MSM?*’, JHEP 10 (2007) 015 [[arXiv:0705.1729](#)]. K. Bondarenko, A. Boyarsky, D. Gorbunov, O. Ruchayskiy, ‘*Phenomenology of GeV-scale Heavy Neutral Leptons*’ [[arXiv:1805.08567](#)].
- [21] A. Atre, T. Han, S. Pascoli, B. Zhang, ‘*The Search for Heavy Majorana Neutrinos*’, JHEP 05 (2009) 030 [[arXiv:0901.3589](#)].
- [22] M. Dittmar, A. Santamaria, M.C. Gonzalez-Garcia, J.W.F. Valle, ‘*Production Mechanisms and Signatures of Isosinglet Neutral Heavy Leptons in Z^0 Decays*’, Nucl.Phys.B 332 (1990) 1.
- [23] FASER Collaboration, ‘*FASER physics reach for long-lived particles*’, Phys.Rev.D 99 (2019) 095011 [[arXiv:1811.12522](#)].
- [24] M. Ovchinnikov, J.-L. Tastet, O. Mikulenko, K. Bondarenko, ‘*Sensitivities to feebly interacting particles: public and unified calculations*’ [[arXiv:2305.13383](#)].
- [25] MATHUSLA Collaboration, ‘*Long-Lived Particles at the Energy Frontier: The MATHUSLA Physics Case*’, Rept.Prog.Phys. 82 (2019) 116201 [[arXiv:1806.07396](#)].

- [26] Z.S. Wang, K. Wang, ‘[Physics with far detectors at future lepton colliders](#)’, Phys.Rev.D 101 (2020) 075046 [[arXiv:1911.06576](#)].
- [27] M. Hirsch, Z.S. Wang, ‘[Heavy neutral leptons at ANUBIS](#)’, Phys.Rev.D 101 (2020) 055034 [[arXiv:2001.04750](#)].
- [28] A. Boyarsky, O. Mikulenko, M. Ovchinnikov, L. Shchutska, ‘[Exploring the potential of FCC-hh to search for particles from B mesons](#)’, JHEP 01 (2023) 042 [[arXiv:2204.01622](#)].
- [29] J.M. Butterworth, M. Chala, C. Englert, M. Spannowsky, A. Titov, ‘[Higgs phenomenology as a probe of sterile neutrinos](#)’, Phys.Rev.D 100 (2019) 115019 [[arXiv:1909.04665](#)].
- [30] G. Cottin, J.C. Helo, M. Hirsch, A. Titov, Z.S. Wang, ‘[Heavy neutral leptons in effective field theory and the high-luminosity LHC](#)’, JHEP 09 (2021) 039 [[arXiv:2105.13851](#)].
- [31] R. Calaga, “Crab Cavities for the High-luminosity LHC”, contribution to SRF17.